

This discussion paper is/has been under review for the journal Biogeosciences (BG).
Please refer to the corresponding final paper in BG if available.

First on-line isotopic characterization of N₂O emitted from intensively managed grassland

B. Wolf^{1,2}, L. Merbold³, C. Decock³, B. Tuzson¹, E. Harris¹, J. Six³,
L. Emmenegger¹, and J. Mohn¹

¹Laboratory for Air Pollution/Environmental Technology, Empa, Überlandstrasse 129, 8600 Dübendorf, Switzerland

²Institute for Meteorology and Climate Research (IMK-IFU), Karlsruhe Institute of Technology, Kreuzackbahnstrasse 19, 82467 Garmisch-Partenkirchen, Germany

³Department of Environmental Systems Science, Swiss Federal Institute of Technology, ETH Zurich, Tannenstrasse 1, 8092 Zürich, Switzerland

Received: 9 December 2014 – Accepted: 22 December 2014 – Published: 23 January 2015

Correspondence to: B. Wolf (benjamin.wolf@kit.edu)

Published by Copernicus Publications on behalf of the European Geosciences Union.

Title Page

Abstract

Introduction

Conclusions

References

Tables

Figures



Back

Close

Full Screen / Esc

Printer-friendly Version

Interactive Discussion



Abstract

The analysis of the four main isotopic N₂O species (¹⁴N¹⁴N¹⁶O, ¹⁴N¹⁵N¹⁶O, ¹⁵N¹⁴N¹⁶O, ¹⁴N¹⁴N¹⁸O) and especially the intramolecular distribution of ¹⁵N (site preference, SP) has been suggested as a tool to distinguish source processes and to help constrain the global N₂O budget. However, current studies suffer from limited spatial and temporal resolution capabilities due to the combination of discrete flask sampling with subsequent laboratory-based mass spectrometric analysis. Quantum cascade laser absorption spectroscopy (QCLAS) allows selective high-precision analysis of N₂O isotopic species at trace levels and is suitable for in situ measurements.

Here, we present results from the first field campaign, conducted on an intensively managed grassland in central Switzerland. N₂O mole fractions and isotopic composition were determined in the atmospheric surface layer (2 m height) at high temporal resolution with a modified state-of-the-art laser spectrometer connected to an automated N₂O preconcentration unit. The analytical performance was determined from repeated measurements of a compressed air tank and resulted in measurement repeatability of 0.20, 0.12 and 0.11‰ for $\delta^{15}\text{N}^{\alpha}$, $\delta^{15}\text{N}^{\beta}$ and $\delta^{18}\text{O}$, respectively. Simultaneous eddy-covariance N₂O flux measurements were used to determine the flux-averaged isotopic signature of soil-emitted N₂O.

Our measurements indicate that in general, nitrifier-denitrification and denitrification were the prevalent sources of N₂O during the campaign, and that variations in isotopic composition were rather due to alterations in the extent to which N₂O was reduced to N₂, than other pathways such as hydroxylamine oxidation. Management and rewetting events were characterized by low values of the intra-molecular ¹⁵N site preference (SP), $\delta^{15}\text{N}^{\text{bulk}}$ and $\delta^{18}\text{O}$, suggesting nitrifier denitrification and incomplete heterotrophic bacterial denitrification responded most strongly to the induced disturbances. Flux-averaged isotopic composition of N₂O from intensively managed grassland was 6.9 ± 4.3 , -17.4 ± 6.2 and 27.4 ± 3.6 ‰ for SP, $\delta^{15}\text{N}^{\text{bulk}}$ and $\delta^{18}\text{O}$, respectively. The approach presented here is capable of providing long-term

BGD

12, 1573–1611, 2015

Real-time grassland N₂O isotopic signature

B. Wolf et al.

Title Page

Abstract

Introduction

Conclusions

References

Tables

Figures



Back

Close

Full Screen / Esc

Printer-friendly Version

Interactive Discussion



datasets also for other N₂O emitting ecosystems, which can be used to further constrain global N₂O inventories.

1 Introduction

Atmospheric nitrous oxide (N₂O) mole fraction is increasing since pre-industrial times predominately due to increased agricultural activity (Davidson, 2009; Mosier et al., 1998). Owing to the approximately 300 times higher global warming potential (GWP) compared to CO₂, this greenhouse gas (GHG) currently accounts for 6% of total anthropogenic radiative forcing (Myhre et al., 2013). Recent estimates showed that N₂O is in addition the single most important ozone-depleting substance (Ravishankara et al., 2009). Because at least 60% of total anthropogenic N₂O emissions is attributed to food production (Syakila and Kroeze, 2011), growing human population and meat consumption per capita as well as biofuel production will accelerate the rate of increase in atmospheric N₂O concentration. Hence, the development of adequate mitigation strategies is pertinent and requires a better understanding of the processes driving N₂O fluxes. To date, nitrification, nitrifier denitrification and denitrification are considered to constitute the dominant N₂O producing processes, especially in agricultural soils (Wrage et al., 2001). Other N₂O source-processes such as abiotic N₂O production, co-denitrification and heterotrophic nitrification have also been observed; a concise overview of observed processes is given elsewhere (Butterbach-Bahl et al., 2013). This complexity inherent in the N cycle and associated transformation processes is a major challenge in developing mitigation strategies, as attribution of N₂O production to the respective processes is required to tailor target-oriented actions (Baggs, 2008). Approaches for apportioning of N₂O emissions to nitrification, denitrification, and N₂O reduction to N₂ (source partitioning) have mostly relied on acetylene (C₂H₂) inhibition and isotope labeling (Groffman et al., 2006), but denitrification rates are underestimated by the C₂H₂ method (Butterbach-Bahl et al., 2013; Groffman et al., 2006; Watts and Seitzinger, 2000). Isotope labeling approaches are vulnerable to

Real-time grassland N₂O isotopic signature

B. Wolf et al.

Title Page

Abstract

Introduction

Conclusions

References

Tables

Figures



Back

Close

Full Screen / Esc

Printer-friendly Version

Interactive Discussion



incomplete diffusion of the tracer and to stimulation of process rates by the addition of the labeled substrates themselves (Groffman et al., 2006). Changes in natural abundance of ^{15}N and ^{18}O in N_2O have been explored to investigate N_2O production processes, but the determined $\delta^{15}\text{N}$ and $\delta^{18}\text{O}$ depend on both fractionation factors and isotopic composition of precursors, which in turn exhibit strong variations (Baggs, 2008; Bedard-Haughn et al., 2003; Heil et al., 2014; Toyoda et al., 2011).

N_2O is a linear molecule and four main isotopic species can be discerned: $^{14}\text{N}^{14}\text{N}^{16}\text{O}$, $^{14}\text{N}^{15}\text{N}^{16}\text{O}$, $^{15}\text{N}^{14}\text{N}^{16}\text{O}$ and $^{14}\text{N}^{14}\text{N}^{18}\text{O}$. The isotopic species $^{14}\text{N}^{14}\text{N}^{16}\text{O}$, $^{14}\text{N}^{14}\text{N}^{18}\text{O}$ and $^{14}\text{N}^{15}\text{N}^{16}\text{O}$ (or $^{15}\text{N}^{14}\text{N}^{16}\text{O}$) are isotopologues, while $^{14}\text{N}^{15}\text{N}^{16}\text{O}$ and $^{15}\text{N}^{14}\text{N}^{16}\text{O}$ are isotopomers and will be termed $^{15}\text{N}^\alpha\text{-N}_2\text{O}$ and $^{15}\text{N}^\beta\text{-N}_2\text{O}$ (Toyoda and Yoshida, 1999). The umbrella term isotopocule is used for both isotopomers and isotopologues. The intra-molecular distribution of ^{15}N in N_2O ("site preference"; $\text{SP} = \delta^{15}\text{N}^\alpha - \delta^{15}\text{N}^\beta$) has been reported to be independent of the substrate's isotopic composition, as SP remained constant even though $\delta^{15}\text{N}$ and $\delta^{18}\text{O}$ values of both N_2O and substrates changed markedly during experiments with pure cultures (Heil et al., 2014; Sutka et al., 2003, 2006, 2008; Toyoda et al., 2005). Therefore, SP can be considered as a tracer conserving the source process information (Ostrom and Ostrom, 2011). The SP of different processes has been characterized in a number of pure-culture, mixed culture (Ostrom et al., 2007; Sutka et al., 2003, 2006; Toyoda et al., 2005; Wunderlin et al., 2012, 2013), and soil-incubation studies (Köster et al., 2011, 2013a; Lewicka-Szczebak et al., 2014; Well et al., 2006, 2008) with a compilation of data in Toyoda et al. (2011). A recent review on source partitioning and SP (Decock and Six, 2013) concluded that SP is capable of distinguishing between the process groups $\text{N}_2\text{O}_\text{N}$ (NH_2OH -oxidation, fungal denitrification and abiotic N_2O production; $\text{SP} = 32.8 \pm 4.0\text{‰}$) and $\text{N}_2\text{O}_\text{D}$ (nitrifier-denitrification and denitrification; $\text{SP} = -1.6 \pm 3.8\text{‰}$). In addition, the intramolecular distribution of ^{15}N can be used as an independent validation of the global, measurement-based bottom-up N_2O budget and has already confirmed that the isotopically light sources such as agriculture and industry contribute to the increase in atmospheric N_2O (Toyoda et al., 2013; Yoshida

BGD

12, 1573–1611, 2015

Real-time grassland N_2O isotopic signature

B. Wolf et al.

Title Page

Abstract

Introduction

Conclusions

References

Tables

Figures



Back

Close

Full Screen / Esc

Printer-friendly Version

Interactive Discussion



and Toyoda, 2000). Owing to the temporal and spatial variability of isotopomer ratios, it is indispensable to derive flux-weighted average values from different sources (such as ecosystems) for later use in budget analysis using box models (Kim and Craig, 1993; Perez et al., 2001; Yoshida and Toyoda, 2000).

Intramolecular distribution of ^{15}N in N_2O can be measured by mass spectrometry, but it requires discrete flask sampling with subsequent laboratory analysis. Hence, this approach is limited in temporal and spatial resolution. Additionally it is indirect, as information on the site-specific isotopic composition is derived from the analysis of the NO^+ fragment and N_2O^+ molecular ion. Recently, a quantum cascade laser absorption spectrometer (QCLAS) capable of selective analysis of the three most abundant N_2O isotopocules has been presented (Waechter et al., 2008) and its potential for in situ measurements in conjunction with an automated pre-concentration unit has been shown (Mohn et al., 2010, 2012). Here we present the results obtained from a, to our knowledge worldwide first, campaign in which the isotopic composition of N_2O (SP, $\delta^{15}\text{N}$, $\delta^{18}\text{O}$) in the atmospheric surface layer was determined on-line by using an optimized state-of-the-art laser spectrometer. With the combination of N_2O isotopic analysis by QCLAS, accompanying eddy-covariance based N_2O flux measurements as well as monitoring of environmental conditions and inorganic nitrogen concentrations, our specific objectives for this study were: (i) to demonstrate the capability of QCLAS systems for high precision isotopic analysis of (soil emitted) N_2O in ambient air, (ii) to investigate management and weather effects on isotopic composition and source processes, (iii) to test the capability of the N_2O isotopic composition for source partitioning, and (iv) to characterize the flux-averaged isotopic composition of N_2O emitted from an intensively managed grassland.

BGD

12, 1573–1611, 2015

Real-time grassland N_2O isotopic signature

B. Wolf et al.

Title Page

Abstract

Introduction

Conclusions

References

Tables

Figures

◀

▶

◀

▶

Back

Close

Full Screen / Esc

Printer-friendly Version

Interactive Discussion



2 Material and methods

2.1 Study site

The agricultural research station Chamau (CHA) is located in Central Switzerland at an elevation of 400 m a.s.l. The experiment was conducted on an intensively managed grassland belonging to CHA which is primarily used for fodder production and occasional winter grazing by sheep (Zeeman et al., 2010). The soil type is a cambisol with a pH of 5–5.5 (Roth, 2006). Mean annual temperature and annual precipitation are 9.1 °C and 1151 mm, respectively (Merbold et al., 2014). Management practices aim at fodder production and consist of mowing followed by slurry application, with up to six mowing/slurry applications per year and occasional grazing of sheep and cattle in October and November. During the campaign in summer 2013, three management cycles were carried out. Harvest dates were 6 June, 11 July and 21 August and slurry was applied within 10 days after each mowing event. Nitrogen input was calculated from the applied amount of slurry brought to the field and the N concentration determined (Labor für Boden- und Umweltanalytik, Eric Schweizer AG, Thun, Switzerland) in a sample drawn from the supply to the trailing hose applicator. The applied N amounted to 30, 40 and 43.3 kg N ha⁻¹ for the first, second and third application, respectively. The grassland is re-established via ploughing and resowing approximately every 10 years. The last re-establishment event took place in 2012.

2.2 Instrumental setup for analysis of N₂O isotopocule ratios

The four most abundant N₂O isotopic species were quantified using a modified QCLAS (Aerodyne Research Inc., Billerica MA, USA) equipped with a continuous wave quantum cascade laser (cw-QCL) with spectral emission at 2203 cm⁻¹, an astigmatic Herriott multi-pass absorption cell (204 m path length, AMAC-200), and reference path with a short (5 cm) N₂O-filled cell to lock the laser emission frequency (Tuzson et al., 2013). During the campaign, the QCLAS was operated in an air-conditioned trailer

BGD

12, 1573–1611, 2015

Real-time grassland
N₂O isotopic
signature

B. Wolf et al.

Title Page

Abstract

Introduction

Conclusions

References

Tables

Figures

◀

▶

◀

▶

Back

Close

Full Screen / Esc

Printer-friendly Version

Interactive Discussion



located 60 m west of the eddy-covariance (EC) tower. This trailer position contributes < 20 % to the main flux and is at the far side of prevailing wind direction (Zeeman et al., 2010). The sample air inlet was installed next to the inlet of the EC tower (2 m height). Sample air was drawn through a PTFE tube (4 mm ID) by a membrane pump (PM 25032-022, KNF Neuberger, Switzerland). Upstream of the pump, the sample air was pre-dried with a permeation drier (MD-050-72S-1, PermaPure Inc., USA). Following the pump, the pressure was maintained at 4 bar overpressure using a pressure relieve valve. Humidity, as well as CO₂, were quantitatively removed from the gas flow by applying a chemical trap filled with Ascarite (7 g, 10–35 mesh, Fluka, Switzerland) bracketed by Mg(ClO₄)₂ (2 × 1.5 g, Fluka, Switzerland). Finally, the sample gas was passed through a sintered metal filter (SS-6F-MM-2, Swagelok, USA) and directed to a preconcentration unit described in detail previously (Mohn et al., 2010, 2012). For an increase of N₂O mixing ratios from ambient level to around 50 ppm N₂O, approx. 8 L of ambient air were preconcentrated. Afterwards, the preconcentrated N₂O was introduced into the evacuated multi-pass cell of the QCLAS. Isotopic fractionation during preconcentration (0.31 ± 0.10, 0.34 ± 0.16 and 0.29 ± 0.07 ‰ for δ¹⁵N^α, δ¹⁵N^β and δ¹⁸O, respectively) was quantified by preconcentration of N₂O with a known isotopic composition and subsequently corrected. Compatibility of N₂O isotopomer analysis by QCLAS with isotope ratio mass spectrometry (IRMS) laboratories was recently demonstrated in an inter-laboratory comparison campaign (Mohn et al., 2014).

2.3 Measurement and calibration strategy

To ensure high accuracy and repeatability of the analytical system, a measurement and calibration strategy similar to the one presented by Mohn et al. (2012) was applied. It is based on two standard gases differing in N₂O isotopic composition, which were produced by dynamic dilution of pure medical N₂O (Pangas, Switzerland) with defined amounts of isotopically pure (> 98 %) ¹⁴N¹⁵N¹⁶O (Cambridge Isotope Laboratories, USA) and (> 99.95 %) and ¹⁴N¹⁴NO (ICON Services Inc., USA). Subsequent gravimetric dilution with high purity synthetic air (99.999 %, Messer

**Real-time grassland
N₂O isotopic
signature**

B. Wolf et al.

Title Page

Abstract

Introduction

Conclusions

References

Tables

Figures



Back

Close

Full Screen / Esc

Printer-friendly Version

Interactive Discussion



Schweiz AG) resulted in pressurized gas mixtures with 90 ppm N₂O (parts per million, 10⁻⁶ mol of trace gas per mole of dry air). Both standards were calibrated against primary standards which were previously measured by the Tokyo Institute of Technology (TIT, Toyoda and Yoshida) to anchor δ values to the international isotopic standard scales. The first standard (S1, Table 1) was used as an anchor point to the international δ scale and used as input data for data analysis algorithms (see data processing). Therefore, the N₂O isotopic composition of S1 was targeted to closely resemble background air. As the N₂O isotopic composition of surface layer air is mainly a mixture of soil-derived and background composition, the second standard (S2, Table 1) used for span correction was depleted in $\delta^{15}\text{N}^\alpha$, $\delta^{15}\text{N}^\beta$ and $\delta^{18}\text{O}$ compared to background air in accordance with the expected terrestrial source signatures.

The measurement protocol started with the injection of S1, dynamically diluted to 50 ppm, the mole fraction of ambient N₂O after preconcentration. After flushing the absorption cell with synthetic air, S2 was injected, also diluted to 50 ppm. For determination of the slight concentration dependence already reported (Mohn et al., 2012), S1 was injected again but at a higher mole fraction of 67 ppm (later referred to as S1_h). This mole fraction represents the mole fraction expected after preconcentration of high concentration surface layer air. Subsequently, S1 was injected again, diluted to 50 ppm, before the cell was filled with preconcentrated ambient N₂O (A). This subroutine (S1 + A) of injection of S1 and preconcentrated ambient N₂O took 35 min and was repeated three times. For an independent determination of repeatability, the fourth sample was preconcentrated compressed air (target gas). During the campaign, two compressed air cylinders (C1 and C2, referred to as target gas) were used. Isotopic composition and N₂O mixing ratio of both cylinders were determined in the laboratory prior to campaign start (Table 1). N₂O mole fractions and isotopic composition analysed in the laboratory and at the field site agreed within their analytical uncertainty. Following target gas analysis, S1 and S1_h were analyzed again. Another set of three subroutines S1 + A completed one run. One complete cycle of 6 ambient air samples and one compressed air sample took 340 min, leading to approx. 25 ambient air samples

**Real-time grassland
N₂O isotopic
signature**

B. Wolf et al.

Title Page

Abstract

Introduction

Conclusions

References

Tables

Figures



Back

Close

Full Screen / Esc

Printer-friendly Version

Interactive Discussion



being analysed during 24 h. N₂O mole fractions were determined according to Mohn et al. (2012).

2.4 Data processing

Data processing is based on individual mixing ratios of the four main N₂O isotopic species and spectrometer characteristics as recorded by the instruments's software (TDLWintel, Aerodyne Research Inc., Billerica, MA, USA). In the first step, variations in the isotope ratios induced by drifts in the instrument working parameters during the field operation were corrected. A linear additive model explaining the deviation of isotope ratios R^α , R^β and $R^{18\text{O}}$ for repeated measurements of standard S1 from their mean value by absorption cell temperature (T1), laser temperature (T2), line position (LP) and pressure (p) was calibrated based on S1 injections. For isotope ratios of S1, S1_h, S2, sample air and compressed air, these systematic deviations were corrected based on the respective values of T1, T2, LP and p . In a second step, concentration dependence of isotope ratios, determined using the measurements of S1 and S1_h, was addressed with corrections (0.013, 0.028 and 0.004 ‰ppb⁻¹ for $\delta^{15}\text{N}^\alpha$, $\delta^{15}\text{N}^\beta$ and $\delta^{18}\text{O}$) being in the same range as described earlier (Mohn et al., 2012). Subsequently, remaining drifts were corrected based on analysis of S1. Finally, isotope ratios were converted to δ values using a 2-point calibration derived from corrected values of S1 and S2.

2.5 Determination of soil-emitted N₂O isotopic composition

Isotopic composition of the source process “soil N₂O emission” was derived using the Keeling plot approach (Keeling, 1958), where δ values measured (here in 2 m height) are plotted vs. the inverse of N₂O mole fractions. The intercept of the linear regression line can be interpreted as the isotopic composition of soil emitted N₂O (Pataki et al., 2003). Therefore, determination of soil N₂O isotopic composition requires an increase in N₂O mole fraction. During the day, turbulence mixes surface layer

BGD

12, 1573–1611, 2015

Real-time grassland N₂O isotopic signature

B. Wolf et al.

Title Page

Abstract

Introduction

Conclusions

References

Tables

Figures



Back

Close

Full Screen / Esc

Printer-friendly Version

Interactive Discussion



air to the atmospheric background. At night, the surface layer becomes more stable and the N₂O mole fraction increases, shifting isotopic composition towards its source composition. As a consequence, Keeling plots were based on noon-to-noon periods. This approach is discussed in Sect. 4.6.

2.6 N₂O Flux measurement

At CHA, greenhouse gas mole fractions, including N₂O, are measured continuously since 2012 by means of the eddy covariance (EC) method (Baldocchi and Meyers, 1998). The system consists of a three-dimensional sonic anemometer to measure wind speed and direction (2 m height, Solent R3, Gill Instruments, Lymington, UK) and a QCLAS (mini-QCLAS, Aerodyne Research Inc., Billerica, MA, USA) to determine N₂O mole fractions at a temporal resolution of 10 Hz. Both data streams are merged near-real time within a data acquisition system (MOXA embedded Linux computer; Moxa, Brea, CA, USA) via an RS-232 serial data link (Eugster and Plüss, 2010). The setup has been described in detail previously (Merbold et al., 2014). Post-processing of N₂O fluxes included screening for obvious out-of-range values ($\pm 100 \text{ nmol m}^{-2} \text{ s}^{-1}$). N₂O fluxes were further aggregated to noon-to-noon daily averages to smoothen the large variability in the 30 min flux averages. Daily averages were calculated for days where more than 30 half-hour values were available, with this filter excluding three days from analysis.

2.7 Soil inorganic N and environmental conditions

Ammonium (NH₄⁺) and nitrate (NO₃⁻) concentrations were determined from soil (0–20 cm depth) sampled at 10 positions along a transect within the footprint of the EC measurements following the predominant wind direction. Samples were taken weekly throughout the campaign or daily during mowing and slurry application events. Per sample, ~ 15 g of fresh soil were added to specimen vessels containing 50 mL 1 M

BGD

12, 1573–1611, 2015

Real-time grassland N₂O isotopic signature

B. Wolf et al.

Title Page

Abstract

Introduction

Conclusions

References

Tables

Figures

⏪

⏩

◀

▶

Back

Close

Full Screen / Esc

Printer-friendly Version

Interactive Discussion



KCl. After 1 h on a shaker, the supernatant was filtered (Whatman no. 42 ashless filter paper, 150 mm diameter) and analysed colorimetrically for NH_4^+ and NO_3^- .

Soil temperatures and volumetric soil moisture contents at 10 cm depth were measured at the same 10 locations along the transect (5TM-sensors, Decagon Devices Ltd., Pullman, USA). Data were stored as 10 min averages on a data logger (EM50, Decagon Devices Ltd., Pullman, USA). The volumetric water content was converted to water filled pore space (wfps) using a bulk density of 1.09 g cm^{-3} . Precipitation was measured with a tipping bucket rain gauge (Type 10116, Toss GmbH, Potsdam, Germany) and stored as 10 min averages on a data logger (CR10X-2M, Campbell Scientific Inc., Logan, USA).

3 Results

3.1 Long term precision for target gas analysis

System performance for N_2O mole fractions and isotopic composition was determined based on repeated analysis of compressed air from target gas tanks (C1, C2). There was no significant drift in the δ values and N_2O mole fractions, indicating stability of the applied measurement technique. Repeatability, calculated as the SD (σ) of 331 target gas measurements, amounted to 0.20, 0.12, 0.10, 0.12 and 0.22 ‰ for $\delta^{15}\text{N}^\alpha$, $\delta^{15}\text{N}^\beta$, $\delta^{18}\text{O}$, $\delta^{15}\text{N}^{\text{bulk}}$ and SP, respectively (Fig. 1). SD for the N_2O mole fraction of the target gas was 0.25 ppb.

3.2 N_2O mole fractions and isotopic composition at 2 m height

N_2O isotopic composition of the surface layer (lowest tens of meters above ground) air samples ($n = 2130$) ranged from 2.5 to 16.1, -11.9 to -2.4 , 37.6 to 44.6, -4.6 to 6.6, and 14.3 to 19.3 ‰ for $\delta^{15}\text{N}^\alpha$, $\delta^{15}\text{N}^\beta$, $\delta^{18}\text{O}$, $\delta^{15}\text{N}^{\text{bulk}}$ and SP, respectively (Fig. 2). Surface layer N_2O mole fractions varied between 325 and 469 ppb and followed

BGD

12, 1573–1611, 2015

**Real-time grassland
 N_2O isotopic
signature**

B. Wolf et al.

Title Page

Abstract

Introduction

Conclusions

References

Tables

Figures

◀

▶

◀

▶

Back

Close

Full Screen / Esc

Printer-friendly Version

Interactive Discussion



a diurnal cycle with highest values during the night when the boundary layer became more stable. Increasing N_2O mole fractions were associated with decreasing δ values, indicating that soil emitted N_2O that mixed into the surface layer was depleted in ^{15}N as compared to N_2O in the atmospheric background.

3.3 Auxiliary measurements

Half hourly N_2O fluxes were averaged from noon-to-noon (f_{N_2O}), and ranged from -1 to $5 \text{ nmol m}^{-2} \text{ s}^{-1}$. Maximum N_2O fluxes coincided with an overnight build up in N_2O mole fractions (ΔN_2O) as analysed by QCLAS and could not be attributed to slurry application events alone (Fig. 3). Among the correlations of f_{N_2O} and auxiliary variables, only the one with nitrate concentration ($r^2 = 0.18$) was significant ($p < 0.01$). Soil water content (wfps) was modulated by precipitation and two clear states could be identified. During the “wet” part of the campaign lasting until 7 July, average wfps was with $62 \pm 4 \%$ significantly (t test, $p < 0.001$) higher than the average of $37 \pm 4 \%$ calculated for the remainder of the campaign (referred to as the “dry” part). Soil temperature did not show such a clear two-phase pattern, however temperatures during the first, “wet” part were with $16.7 \pm 4^\circ\text{C}$ significantly ($p < 0.001$) lower than during the “dry” phase with $21.2 \pm 2^\circ\text{C}$.

Background NH_4^+ and NO_3^- concentrations were smaller than $3 \mu\text{g g}_{\text{soil}}^{-1}$ and clearly responded to mowing and slurry application in the second and third management events. The NO_3^- concentration was higher than the NH_4^+ concentration and peaked at 16 and $50 \mu\text{g g}_{\text{soil}}^{-1}$, while NH_4^+ concentration peaked at 9 and $15 \mu\text{g g}_{\text{soil}}^{-1}$ for these two management events. In contrast, dissolved organic carbon concentrations (DOC) did not respond to management events, but were higher during the “dry” phase of the campaign ($p < 0.001$).

BGD

12, 1573–1611, 2015

Real-time grassland N_2O isotopic signature

B. Wolf et al.

Title Page

Abstract

Introduction

Conclusions

References

Tables

Figures

◀

▶

◀

▶

Back

Close

Full Screen / Esc

Printer-friendly Version

Interactive Discussion



3.4 Isotopic composition of soil-emitted N₂O

The uncertainty of the determined source isotopic composition was estimated based on the standard error of the Keeling plot intercept and depends on the degree to which soil air accumulated in the surface layer (ΔN_2O , Fig. 4). For instance, the intercept (source) standard error ranged from 0.3 to 82‰ for SP. To apply the Keeling plot approach only to situations in which soil air accumulated in the surface layer, only source isotopic compositions for overnight increases in N₂O mole fractions of more than 12 ppb were considered in this study. This filter lead to a maximum and average (μ) standard error of 6.8 ($\mu = 2.2$), 4.5 ($\mu = 1.4$) and 2.2 ($\mu = 1$)‰ for SP, $\delta^{15}N^{bulk}$ and $\delta^{18}O$ isotopic source signatures, respectively.

During the field campaign, Keeling plot derived isotopic composition of soil-emitted N₂O ranged from 1.4 to 17.3, -29 to -3 and 22.6 to 34.8‰ for SP, $\delta^{15}N^{bulk}$ and $\delta^{18}O$, respectively. All explanatory variables except NH₄⁺ and NO₃⁻ were found to significantly correlate with SP (Table 2). For $\delta^{15}N^{bulk}$, correlations with ΔN_2O , wfps, soil temperature, DOC and NO₃⁻ and for $\delta^{18}O$ correlations of f_{N_2O} , ΔN_2O , precipitation, soil temperature and NO₃⁻ were significant. However, the adjusted r^2 for all regressions was below 0.4; in addition, multiple explanatory variables such as NH₄⁺ and NO₃⁻ or wfps and temperature (Fig. 5) did not increase the explained variance above this value.

3.5 Event-based data aggregation

As already described in Sect. 3.3, there was a “wet” phase ($n = 27$) in the beginning of the campaign, which lasted about one month and a “dry” phase lasting about two months ($n = 38$). Therefore, the dataset was split in two corresponding parts with averages of 7.4 ± 3.6 vs. 11.1 ± 4.2 ‰ for SP, -19 ± 3.8 vs. -12.5 ± 5.9 ‰ for $\delta^{15}N^{bulk}$ and 28.7 ± 2.2 vs. 29.7 ± 3.4 ‰ for $\delta^{18}O$ in the wet vs. the dry phase, respectively. Averages of SP and $\delta^{15}N^{bulk}$ were significantly different ($p < 0.001$) but $\delta^{18}O$ averages were not. Based on this simple classification, the dry phase contains rewetting events.

A rewetting event was defined as a two day period starting at the day for which wfps increased. Exclusion of these rewetting events during the dry phase increased average δ -values ($n = 30$) as well as decreased SDs for SP, $\delta^{15}\text{N}^{\text{bulk}}$ and $\delta^{18}\text{O}$ to 12.5 ± 3.4 , -10.8 ± 4.5 and $30.7 \pm 2.8\%$. Moreover the difference in $\delta^{18}\text{O}$ was significant ($p < 0.001$).

In addition to the dry/wet classification, we also defined three subsets representing the N_2O emission associated with management events of mowing followed by fertilization (“Mana I”–“Mana III”), one subset representing a rewetting event between Mana II and III (“Rewetting”) and one subset representing background (“BG”, all remaining measurements). There were two distinct rewetting events between management events II and III, but N_2O isotopic composition is only available for the first one (29–31 July 2014). Isotopic compositions of soil-emitted N_2O were assigned to subsets of management or rewetting if the associated flux or nutrient concentration was elevated. This classification scheme led to 3–7 measurements for management and rewetting events (Fig. 3, underlaid in transparent blue) while 47 measurements were assigned to class BG. Boxplots for SP, $\delta^{15}\text{N}^{\text{bulk}}$, $\delta^{18}\text{O}$, and wfps (Fig. 6) showed characteristic δ -values and wfps for management and rewetting, but not for subset BG. Measurements assigned to BG covered practically the whole range of values observed across all the other classes. Therefore, SDs for class BG were one order of magnitude larger than for the four other classes.

Statistical analysis is confounded by low and unequal sample size so that we compared exclusively the subsets management and rewetting using multiple non-parametric Wilcoxon tests after having checked homogeneity of variances using Bartlett test. For all investigated δ -values, only differences between groups Mana II and Mana III were significant.

BGD

12, 1573–1611, 2015

Real-time grassland N_2O isotopic signature

B. Wolf et al.

Title Page

Abstract

Introduction

Conclusions

References

Tables

Figures

◀

▶

◀

▶

Back

Close

Full Screen / Esc

Printer-friendly Version

Interactive Discussion



3.6 Averages of N₂O isotopic signature for intensively managed grassland

Simple averages of daily isotopic composition of soil-emitted N₂O were 9.6 ± 4.4 , -15.2 ± 6.0 and $29.3 \pm 3\%$ for SP, $\delta^{15}\text{N}^{\text{bulk}}$ and $\delta^{18}\text{O}$, respectively ($n = 62$). Representative isotopic signature for agricultural land can be estimated based on flux-weighted averages of daily signatures. For some noon-to-noon periods included in the above average, thus with an overnight increase in N₂O mole fractions of at least 12 ppb, negative N₂O fluxes were detected by the EC system ($-0.17 \pm 2.1 \text{ nmol m}^{-2} \text{ s}^{-1}$; $n = 14$). This might be due to the uncertainty of N₂O flux measurements, temporal averaging over positive and negative fluxes in a noon-to-noon period or different footprint regions for N₂O flux and isotopic analysis (flux vs. concentration footprint). To avoid bias to the flux-weighted average of emitted N₂O by either one of the above mentioned possible reasons, the weighted averages were calculated for positive flux events only. Flux weighted averages were 6.9 ± 4.3 , -17.4 ± 6.2 and $27.4 \pm 3.6\%$ for SP, $\delta^{15}\text{N}^{\text{bulk}}$ and $\delta^{18}\text{O}$ respectively ($n = 48$).

4 Discussion

4.1 Analytical performance

To our knowledge, only two pilot studies exist demonstrating the potential of QCLAS based analytical techniques for on-line and high-precision analysis of N₂O mole fractions and isotopic composition in surface layer air. While Mohn et al. (2012) analyzed the three most abundant ¹⁵N-isotopocules (¹⁴N¹⁴N¹⁶O, ¹⁵N¹⁴N¹⁶O, ¹⁴N¹⁵N¹⁶O), Harris et al. (2014) included the ¹⁸O isotopologue (¹⁴N¹⁴N¹⁸O). In both studies, however, the instrument was located in the laboratory. Based on three weeks of measurements, Mohn et al. (2012) reported a precision of 0.24 and 0.17‰ for $\delta^{15}\text{N}^{\alpha}$ and $\delta^{15}\text{N}^{\beta}$, respectively and Harris et al. (2014) reported 0.17, 0.19 and 0.32‰ for $\delta^{15}\text{N}^{\alpha}$, $\delta^{15}\text{N}^{\beta}$ and $\delta^{18}\text{O}$, respectively, for a twelve days period. In both studies,

BGD

12, 1573–1611, 2015

Real-time grassland
N₂O isotopic
signature

B. Wolf et al.

Title Page

Abstract

Introduction

Conclusions

References

Tables

Figures

◀

▶

◀

▶

Back

Close

Full Screen / Esc

Printer-friendly Version

Interactive Discussion



analytical performance was determined, in accordance with the presented study, based on repeated analysis of compressed air samples. Thereby, the analytical precision reached in the presented study, was distinctly higher for $\delta^{15}\text{N}^{\beta}$ and $\delta^{18}\text{O}$ and similar for $\delta^{15}\text{N}^{\alpha}$ compared to these two previous studies, even though the measurements were done under field-conditions and over a much longer, three months, period. This confirms the high level of precision associated with QCLAS based determination of N_2O isotopic composition. Standard errors for Keeling plot intercepts (Fig. 4) confirm that this precision is sufficient to resolve the variability of atmospheric N_2O sampled close to the ground. As our instrument was located directly at the field site and measurements were conducted over a period of more than three months, our study indicates that this level of repeatability can be achieved both at long time scales and in the field.

4.2 N_2O isotopic composition in the atmospheric surface layer (2 m height)

In our study, δ -values of single preconcentrated air samples were between atmospheric background and 14.3‰ (SP) and -4.7‰ ($\delta^{15}\text{N}^{\text{bulk}}$). Mohn et al. (2012) reported similar values between atmospheric background and 12‰ (SP) and -4‰ ($\delta^{15}\text{N}^{\text{bulk}}$). Therefore the variation observed in both studies is much higher compared to the measurements by Harris et al. (2014) where the N_2O isotopic composition deviated only slightly from atmospheric background. A consistent decrease in $\delta^{15}\text{N}^{\text{bulk}}$ in parallel with increasing N_2O mole fractions (accumulation of soil-derived N_2O) confirms that the soil N_2O source is depleted in ^{15}N - N_2O relative to ambient N_2O (Toyoda et al., 2013). A similar pattern was found for $\delta^{18}\text{O}$; an increase in N_2O mole fraction was associated with a decrease in ^{18}O - N_2O , again indicating that soil emissions were depleted in ^{18}O - N_2O with respect to the atmospheric background. In contrast, Harris et al. (2014) reported a decoupling of $\delta^{18}\text{O}$ and $\delta^{15}\text{N}^{\text{bulk}}$. This may have been due to only marginal influence of soil-emitted N_2O since the measurements were carried out in urban area and approx. 95 m above the ground. Studies on N_2O derived from

BGD

12, 1573–1611, 2015

Real-time grassland N_2O isotopic signature

B. Wolf et al.

Title Page

Abstract

Introduction

Conclusions

References

Tables

Figures



Back

Close

Full Screen / Esc

Printer-friendly Version

Interactive Discussion



combustion processes indicate that some of these sources might be less depleted or even enriched in ^{15}N - N_2O compared to ambient N_2O (Harris et al., 2015; Ogawa and Yoshida, 2005).

4.3 Isotopic composition of soil-emitted N_2O

5 SP of soil-emitted N_2O observed in our study (1–17‰) is within the ranges expected for a mixture of the two process groups $\text{N}_2\text{O}_\text{N}$ and $\text{N}_2\text{O}_\text{D}$, and does not necessarily indicate significant contribution of N_2O reduction, an effect which is discussed further below. Isotopic composition of soil-emitted N_2O has been predominately determined in laboratory incubation studies (Köster et al., 2013a, b; Perez et al., 2006; Well and Flessa, 2009b; Well et al., 2006, 2008). Additionally, results from field experiments using static chambers (Opdyke et al., 2009; Ostrom et al., 2010; Toyoda et al., 2011; Yamulki et al., 2001) and N_2O accumulation below a snowpack have been published (Mohn et al., 2013). Based on pure culture studies SP values from 19.7 to 40 and –8.7 to 8.5‰, were observed for $\text{N}_2\text{O}_\text{N}$ and $\text{N}_2\text{O}_\text{D}$, respectively (Decock and Six, 2013). In field experiments SP was found to range between –1 and 32‰ (Opdyke et al., 2009), –3 and 18‰ (Yamulki et al., 2001), –14 and 90‰ (Toyoda et al., 2011) and 0 and 13‰ (Ostrom et al., 2010). The very high SP values detected by Toyoda et al. (2011) may have resulted from extensive N_2O reduction to N_2 , a process increasing SP, $\delta^{15}\text{N}^{\text{bulk}}$ and $\delta^{18}\text{O}$ (Ostrom et al., 2007). For $\delta^{15}\text{N}^{\text{bulk}}$ and $\delta^{18}\text{O}$, a much wider variation as compared to SP is expected, because these variables depend both on fractionation factors, which vary among different microbial communities and depend on reaction conditions, as well as on the isotopic composition of the substrate (Baggs, 2008). Under field conditions, $\delta^{15}\text{N}^{\text{bulk}}$ was reported to range between –17 and 9‰ (Opdyke et al., 2009), –27 and 1‰ (Yamulki et al., 2001), –44 and 34‰ (Toyoda et al., 2011) and –18 and –15‰ (Ostrom et al., 2010), covering the range of –29 to –3‰ observed in this study. With respect to $\delta^{18}\text{O}$, the values of 22.6 to 34.8‰ detected for grassland in this study are at the lower end of measurements under field conditions (4–82‰).

4.4 Changes in N₂O source signatures induced by N₂O reduction to N₂

Quantitative source partitioning between process groups N₂O_N and N₂O_D based on SP is possible only when no other processes except those contained in the process groups have an influence on the site-specific N₂O isotopic composition. However, in the terminal step of denitrification, namely the reduction of N₂O to N₂, where N₂O is the substrate, the lighter isotopic species is consumed, leading to an increase in SP, $\delta^{15}\text{N}^{\text{bulk}}$ and $\delta^{18}\text{O}$. Consequently, part of the N₂O originating from a combination of the two process groups, i.e. N₂O_N and N₂O_D, may have been consumed by N₂O to N₂ reduction prior to emission.

For identification of processes determining N₂O isotopic composition, isotopocule maps were suggested in which site preference is plotted vs. the difference in substrate and product isotopic composition (Koba et al., 2009). Determination of isotopic composition in the substrates is time consuming and additionally confounded in our study by the large and varying footprint area. Therefore, we present a modified isotope map of SP vs. $\delta^{15}\text{N}^{\text{bulk}}$ (Fig. 7) instead of $\Delta\delta^{15}\text{N}$, the $\delta^{15}\text{N}$ differences between substrate and product (i.e. N₂O gas). Rectangles for process groups N₂O_N and N₂O_D are defined by SP values given by Decock and Six (2013) and by $\delta^{15}\text{N}^{\text{bulk}}$ values calculated based on process fractionation factors and substrate isotopic composition. For nitrification and denitrification minimum and maximum fractionation factors of -90 to -40 and -40 to -15‰ were assumed (Baggs, 2008), for the isotopic compositions of the N₂O precursors (i.e., NH₄⁺ and NO₃⁻) a range of -20 to +10 and -25 to 15‰ were assumed. Koba et al. (2009) attributed a concurrent decrease in $\delta^{15}\text{N}^{\text{bulk}}$ with increasing SP values as indicative for an increasing contribution of N₂O_N. In contrast, an increase in $\delta^{15}\text{N}^{\text{bulk}}$ in parallel to increasing SP values (enrichment of ¹⁵N in the α position relative to the β position), as observed in the present study, was allocated to a substantial increase in N₂O reduction to N₂. For $\varepsilon^{15}\text{N}^{\text{bulk}}/\varepsilon\text{SP}$ of N₂O reduction, Koba et al. (2009) assumed a factor of 1.2 based on previous publications. Our results (Fig. 7) indicate that N₂O is predominately formed by denitrification, and that deviations

BGD

12, 1573–1611, 2015

Real-time grassland N₂O isotopic signature

B. Wolf et al.

Title Page

Abstract

Introduction

Conclusions

References

Tables

Figures

◀

▶

◀

▶

Back

Close

Full Screen / Esc

Printer-friendly Version

Interactive Discussion



Real-time grassland N₂O isotopic signature

B. Wolf et al.

[Title Page](#)

[Abstract](#)

[Introduction](#)

[Conclusions](#)

[References](#)

[Tables](#)

[Figures](#)



[Back](#)

[Close](#)

[Full Screen / Esc](#)

[Printer-friendly Version](#)

[Interactive Discussion](#)



in the isotope values from denitrification may have been caused by variations in the extent to which N₂O was reduced to N₂. Additionally, $\delta^{18}\text{O}$ was found to be positively correlated with $\delta^{15}\text{N}^{\text{bulk}}$, which enforces the interpretation that varying shares of N₂O reduction occurred because it acts on both N and O isotopic composition (Koehler et al., 2012). It is noteworthy that based on such modified isotope maps, systematic changes in $\delta^{15}\text{N}^{\text{bulk}}$ induced by systematic changes in N isotopic composition of one of the precursors NH₄⁺ or NO₃⁻ could be misinterpreted as reduction events.

The ratios of fractionation factors for $\delta^{18}\text{O}$ and $\delta^{15}\text{N}^{\text{bulk}}$ ($r_{\text{o-n}}$) and SP and $\delta^{18}\text{O}$ ($r_{\text{sp-o}}$) during N₂O reduction were suggested for estimation of the share of N₂O reduction to N₂ since these ratios were found to be 2.5 and 0.2 to 0.5, respectively in laboratory incubation experiments (Jinuntuya-Nortman et al., 2008; Ostrom et al., 2007; Well and Flessa, 2009a). We calculated these ratios for a subset of data for which all δ -values (SP, $\delta^{15}\text{N}^{\text{bulk}}$ and $\delta^{18}\text{O}$) increased for two consecutive days, indicating that N₂O reduction occurred. Such events were observed on 8 occasions. If source processes (N₂O_D, N₂O_N) contributed constantly over two consecutive measuring days, changes in the isotopic composition of emitted N₂O were solely attributed to changes in the fraction of N₂O reduction. Under such conditions one would expect that the ratio of the changes in $\delta^{18}\text{O}$ and $\delta^{15}\text{N}^{\text{bulk}}$ ($r_{\text{o-n}}$) is around 2.5 and that the ratio of the changes in SP and $\delta^{18}\text{O}$ ($r_{\text{sp-o}}$) is between 0.2 and 0.5. The mean (median) ratios for $r_{\text{o-n}}$ and $r_{\text{sp-o}}$ for these selected events were 0.69 (0.44) and 2.1 (1.16), respectively. While the high values of $r_{\text{sp-o}}$ indicate that for instance changing physical conditions such as soil moisture may play a role in field measurements, the deviation of $r_{\text{o-n}}$ from the value of 2.5 could either indicate that the fractionation factor for ¹⁸O might be smaller than the one for ¹⁵N or that there is no correlation of fractionation factors in natural environments. This is in line with recent findings showing that apparent isotope effects associated with N₂O reduction are sensitive to experimental conditions which influenced diffusive isotope effects (Lewicka-Szczebak et al., 2014). The same study also showed that fractionation factors during N₂O reduction for ¹⁵N and ¹⁸O were variable (from –11 to +12 ‰ and from –18 to +4 ‰, respectively), and not predictable for field conditions yet.

Real-time grassland N₂O isotopic signature

B. Wolf et al.

[Title Page](#)

[Abstract](#)

[Introduction](#)

[Conclusions](#)

[References](#)

[Tables](#)

[Figures](#)



[Back](#)

[Close](#)

[Full Screen / Esc](#)

[Printer-friendly Version](#)

[Interactive Discussion](#)



Therefore, to date, the amount of N₂O reduction prior to emission cannot be inferred with sufficient robustness from field measurements alone, without the knowledge of isotopic composition of the substrates.

4.5 Controls on isotopic composition and event based data aggregation

The high temporal resolution of N₂O isotopic and auxiliary measurements allowed us to investigate controls on N₂O isotopic composition over the 3 months campaign period. Correlations with isotopic composition were highest and positive for DOC and soil temperature (Table 2). The significant correlation with temperature for the whole campaign was due to a significant correlation during the “dry” part of the campaign.

If the increase in SP was due to increased contribution of nitrification, $\delta^{15}\text{N}^{\text{bulk}}$ should decrease due to the higher isotopic fractionation during this process. The simultaneous increase in SP, $\delta^{15}\text{N}^{\text{bulk}}$ and $\delta^{18}\text{O}$ revealed in Fig. 7, however, indicates an increased share of N₂O reduction to N₂ which might have been triggered by increased substrate availability (DOC) for heterotrophic denitrification. The reported effect of temperature on the N₂O : N₂ ratio is not without any doubt, but a decrease has been observed with increasing temperature, supporting the hypothesis that N₂O reduction increased as temperature rose throughout the measurement period (Saggar et al., 2013).

Though substrate availability has been identified as a major control on N₂O source processes (see references in Saggar et al., 2013), correlations between N₂O isotopic composition and NO₃⁻ and NH₄⁺ concentrations were low, except for the correlation with $\delta^{15}\text{N}^{\text{bulk}}$. The reason might be both the number of measurement points for substrate concentrations being lower compared to other explanatory variables and substrate concentrations not necessarily reflecting process or turnover rates (Wu et al., 2012).

The low explanatory power of all linear regressions underlines that drivers for N₂O emissions are highly variable and may even change from event to event. In absence of management or rewetting events (group BG), isotopic composition covered the whole range of measured values, while management or rewetting events were characterized

by lower variability in isotopic composition. Values for SP, $\delta^{15}\text{N}^{\text{bulk}}$ and $\delta^{18}\text{O}$ were low for Mana I, rewetting and Mana III, whereas event Mana II showed increased SP, $\delta^{15}\text{N}^{\text{bulk}}$ and $\delta^{18}\text{O}$. This indicates that processes must have been different for Mana II, although management was almost identical.

5 4.6 Short term variation of isotopic composition

The Keeling plot approach is based on conservation of mass and assumes that the atmospheric concentration of a gas in the surface layer is a mixture of background atmospheric concentration and a variable amount of gas added by a source, raising the atmospheric concentration above background. The source's isotope value can be determined given that its isotope value remains constant during the observation period. In this study, we used noon-to-noon data in the Keeling plots to determine isotope values of soil-derived N_2O for the respective noon-to-noon period. Hence, the source processes underlying these N_2O emissions have to be constant on this time scale. Currently, little is known about the rate of change of N_2O source processes over time-steps of minutes to hours. However, changing relative contributions of source processes, which change the isotopic composition in soil-emitted N_2O , would be reflected by deviations from a linear relation between inverse concentration and isotopic composition. As the Keeling plots showed no obvious deviations from a linear relation within our measurement precision, we conclude (1) that the use of the Keeling plot approach was valid in our study, and (2) that changes in N_2O source processes in our study site occurred at a time step of one day or more. While our data suggests that there are little or no changes in source processes underlying N_2O emissions within a noon-to-noon period, clear and distinct day-to-day variation in isotope values of soil derived N_2O , especially in SP, were observed. Such changes were often strong and abrupt following management events (Mana I and III, Rewetting), indicating a significant response of microbial processes to the imposed disturbance. Larger than expected variability in isotope values was observed in-between management events (class BG),

BGD

12, 1573–1611, 2015

Real-time grassland N_2O isotopic signature

B. Wolf et al.

Title Page

Abstract

Introduction

Conclusions

References

Tables

Figures



Back

Close

Full Screen / Esc

Printer-friendly Version

Interactive Discussion



when no obvious variation in environmental drivers occurred. Since noon-to-noon concentration increases were very small during these periods, part of this variability may be attributed to increased uncertainty around the intercept of the Keeling plot. This is also reflected in the relatively large error bars around isotope values on days when N₂O fluxes were low (Fig. 3). Alternatively some of the variation in isotope values associated with these small fluxes may result from air masses not representative of the grassland site as the concentration footprint influencing the N₂O source signature is larger than the flux footprint (Griffis et al., 2007).

4.7 Flux weighted averages of source isotopic compositions

N₂O isotopic composition can be used to calculate and further constrain the global N₂O budget (Kim and Craig, 1993; Yoshida and Toyoda, 2000). The analysis of emissions from different sources such as agricultural soils or managed grasslands based on box models and isotopic composition is complicated by distinct temporal and spatial variability of isotopic composition (Kim and Craig, 1993; Toyoda et al., 2011; Yoshida and Toyoda, 2000); hence, flux weighted averages are required to obtain representative values for agricultural N₂O (Perez et al., 2001). Our flux weighted averages of 6.9 ± 4.3 , -17.4 ± 6.2 and 27.4 ± 3.6 ‰ for SP, $\delta^{15}\text{N}^{\text{bulk}}$ and $\delta^{18}\text{O}$ are well within the range of values 2.9 to 36.6, -41.5 to -1.9 and 23.2 to 51.7‰ for agricultural soils (Park et al., 2011; Toyoda et al., 2011), but the comparison with other grassland soils (Opdyke et al., 2009; Park et al., 2011) indicates that the variability of isotopic composition within a group, such as grassland, may be considerable (for SP: 2.2 to 11.1‰). Part of the variability might be also explained by a limited compatibility of laboratory results, as recently demonstrated in an inter-laboratory comparison campaign (Mohn et al., 2014). The uncertainty in budgets derived by isotopic composition depends on the uncertainty of the representative isotopic composition for a single source, which can be reduced by a quasi-continuous measurement approach, as shown in this study.

BGD

12, 1573–1611, 2015

Real-time grassland N₂O isotopic signature

B. Wolf et al.

Title Page

Abstract

Introduction

Conclusions

References

Tables

Figures



Back

Close

Full Screen / Esc

Printer-friendly Version

Interactive Discussion



5 Conclusion

Our field observations indicate that nitrifier-denitrification and denitrification (process group N_2O_D) dominated throughout the measurement period and that variation in isotopic composition was more likely due to variation in the extent of N_2O reduction rather than contributions of NH_2OH oxidation. High temporal resolution of isotopic composition in soil-emitted N_2O showed that at the beginning of the growing season, medium wfps and low temperature induced low isotope values (representative for process group N_2O_D), whereas in the second part of the measurement period, higher temperature and DOC stimulated N_2O reduction to N_2 , although wfps was lower. Management or rewetting events were mostly characterized by low SP, $\delta^{15}N^{bulk}$ and $\delta^{18}O$, but the event Mana II indicated that processes underlying N_2O emissions can vary even under similar management conditions. With this study, a new method is available that can provide real-time datasets for various single N_2O emitting (eco)systems, such as as grasslands or agricultural soils, which will help in further constraining the global N_2O budget based on box model calculations.

Acknowledgements. We are grateful to Hans-Ruedi Wettstein and his team for the collaboration with the ETH research station Chamau and Christoph Zellweger for support with determination of GHG mixing ratios in our target gases. Antoine Roth is acknowledged for his support during the field campaign. This project was funded by the State Secretariat for Education and Research (SER) within COST Action ES0806. The QCLAS used for EC measurements was funded by the R'Equip Project (206021 133763) by the Swiss National Science Foundation. Funding from GHG-Europe (FP7, EU contract No. 244122) and COST-ES0804 ABBA is gratefully acknowledged. Instrumental developments at Empa were supported by the Swiss National Science Foundation (SNSF). Technical support on the eddy covariance station has been provided by Thomas Baur and Peter Plüss. Preparation of N_2O isotope standards and inter-laboratory comparison measurements were supported by the EMRP ENV52 project "Metrology for high-impact greenhouse gases". The EMRP is jointly funded by the EMRP participating countries within EURAMET and the European Union.

BGD

12, 1573–1611, 2015

Real-time grassland N_2O isotopic signature

B. Wolf et al.

Title Page

Abstract

Introduction

Conclusions

References

Tables

Figures



Back

Close

Full Screen / Esc

Printer-friendly Version

Interactive Discussion



References

- Baggs, E. M.: A review of stable isotope techniques for N₂O source partitioning in soils?: recent progress, remaining challenges and future considerations, *Rapid Commun. Mass Sp.*, 22, 1664–1672, doi:10.1002/rcm.3456, 2008.
- 5 Baldocchi, D. and Meyers, T.: On using eco-physiological, micrometeorological and biogeochemical theory to evaluate carbon dioxide, water vapor and trace gas fluxes over vegetation: a perspective, *Agr. Forest Meteorol.*, 90, 1–25, doi:10.1016/S0168-1923(97)00072-5, 1998.
- Bedard-Haughn, A., van Groenigen, J. W., and van Kessel, C.: Tracing ¹⁵N through landscapes: potential uses and precautions, *J. Hydrol.*, 272, 175–190, doi:10.1016/S0022-1694(02)00263-9, 2003.
- 10 Butterbach-Bahl, K., Baggs, E. M., Dannenmann, M., Kiese, R., and Zechmeister-Boltenstern, S.: Nitrous oxide emissions from soils?: how well do we understand the processes and their controls?, *Philos. T. R. Soc. B*, 368, 20130122, doi:10.1098/rstb.2013.0122, 2013.
- 15 Davidson, E. A.: The contribution of manure and fertilizer nitrogen to atmospheric nitrous oxide since 1860, *Nat. Geosci.*, 2, 659–662, 2009.
- Decock, C. and Six, J.: How reliable is the intramolecular distribution of ¹⁵N in N₂O to source partition N₂O emitted from soil?, *Soil Biol. Biochem.*, 65, 114–127, doi:10.1016/j.soilbio.2013.05.012, 2013.
- 20 Eugster, W. and Plüss, P.: A fault-tolerant eddy covariance system for measuring CH₄ fluxes, *Agr. Forest Meteorol.*, 150, 841–851, doi:10.1016/j.agrformet.2009.12.008, 2010.
- Griffis, T. J., Zhang, J., Baker, J. M., Kljun, N., and Billmark, K.: Determining carbon isotope signatures from micrometeorological measurements: implications for studying biosphere–atmosphere exchange processes, *Bound.-Lay. Meteorol.*, 123, 295–316, doi:10.1007/s10546-006-9143-8, 2007.
- 25 Groffman, P. M., Altabet, M. A., Bohlke, J. K., Butterbach-Bahl, K., David, M. B., Firestone, M. K., Giblin, A. E., Kana, T. M., Nielsen, L. P., and Voytek, M. A.: Methods for measuring denitrification: diverse approaches to a difficult problem, *Ecol. Appl.*, 16, 2091–2122, 2006.
- 30 Harris, E., Nelson, D. D., Olszewski, W., Zahniser, M., Potter, K. E., McManus, B. J., Whitehill, A., Prinn, R. G., and Ono, S.: Development of a spectroscopic technique for

Title Page

Abstract

Introduction

Conclusions

References

Tables

Figures



Back

Close

Full Screen / Esc

Printer-friendly Version

Interactive Discussion



**Real-time grassland
N₂O isotopic
signature**

B. Wolf et al.

[Title Page](#)[Abstract](#)[Introduction](#)[Conclusions](#)[References](#)[Tables](#)[Figures](#)[Back](#)[Close](#)[Full Screen / Esc](#)[Printer-friendly Version](#)[Interactive Discussion](#)

continuous online monitoring of oxygen and site-specific nitrogen isotopic composition of atmospheric nitrous oxide, *Anal. Chem.*, 86, 1726–1734, doi:10.1021/ac403606u, 2014.

Harris, E., Zeyer, K., Kegel, R., Müller, B., Emmenegger, L., and Mohn, J.: Nitrous oxide emissions and isotopic composition from waste incineration in Switzerland, *Waste Manag.*, 35, 135–140, 2015.

Heil, J., Wolf, B., Brüggemann, N., Emmenegger, L., Tuzson, B., Vereecken, H., and Mohn, J.: Site-specific ¹⁵N isotopic signatures of abiotically produced N₂O, *Geochim. Cosmochim. Ac.*, 139, 72–82, doi:10.1016/j.gca.2014.04.037, 2014.

Jinuntuya-Nortman, M., Sutka, R. L., Ostrom, P. H., Gandhi, H., and Ostrom, N. E.: Isotopologue fractionation during microbial reduction of N₂O within soil mesocosms as a function of water-filled pore space, *Soil Biol. Biochem.*, 40, 2273–2280, doi:10.1016/j.soilbio.2008.05.016, 2008.

Keeling, C. D.: The concentration and isotopic abundances of atmospheric carbon dioxide in rural areas, *Geochim. Cosmochim. Ac.*, 13, 322–334, doi:10.1016/0016-7037(58)90033-4, 1958.

Kim, K. R. and Craig, H.: Nitrogen-15 and oxygen-18 characteristics of nitrous oxide: a global perspective., *Science*, 262, 1855–1857, doi:10.1126/science.262.5141.1855, 1993.

Koba, K., Osaka, K., Tobar, Y., Toyoda, S., Ohte, N., Katsuyama, M., Suzuki, N., Itoh, M., Yamagishi, H., Kawasaki, M., Kim, S. J., Yoshida, N., and Nakajima, T.: Biogeochemistry of nitrous oxide in groundwater in a forested ecosystem elucidated by nitrous oxide isotopomer measurements, *Geochim. Cosmochim. Ac.*, 73, 3115–3133, doi:10.1016/j.gca.2009.03.022, 2009.

Koehler, B., Corre, M. D., Steger, K., Well, R., Zehe, E., Sueta, J. P., and Veldkamp, E.: An in-depth look into a tropical lowland forest soil: nitrogen-addition effects on the contents of N₂O, CO₂ and CH₄ and N₂O isotopic signatures down to 2-m depth, *Biogeochemistry*, 111, 695–713, doi:10.1007/s10533-012-9711-6, 2012.

Köster, J. R., Cárdenas, L., Senbayram, M., Bol, R., Well, R., Butler, M., Mühling, K. H., and Dittert, K.: Rapid shift from denitrification to nitrification in soil after biogas residue application as indicated by nitrous oxide isotopomers, *Soil Biol. Biochem.*, 43, 1671–1677, doi:10.1016/j.soilbio.2011.04.004, 2011.

Köster, J. R., Well, R., Dittert, K., Giesemann, A., Lewicka-Szczebak, D., Mühling, K.-H., Herrmann, A., Lammel, J., and Senbayram, M.: Soil denitrification potential and its influence

Real-time grassland N₂O isotopic signature

B. Wolf et al.

[Title Page](#)
[Abstract](#)
[Introduction](#)
[Conclusions](#)
[References](#)
[Tables](#)
[Figures](#)

[Back](#)
[Close](#)
[Full Screen / Esc](#)
[Printer-friendly Version](#)
[Interactive Discussion](#)


on N₂O reduction and N₂O isotopomer ratios, *Rapid Commun. Mass Sp.*, 27, 2363–2373, doi:10.1002/rcm.6699, 2013a.

Köster, J. R., Well, R., Tuzson, B., Bol, R., Dittert, K., Giesemann, A., Emmenegger, L., Manninen, A., Cárdenas, L., and Mohn, J.: Novel laser spectroscopic technique for continuous analysis of N₂O isotopomers-application and intercomparison with isotope ratio mass spectrometry, *Rapid Commun. Mass Sp.*, 27, 216–222, doi:10.1002/rcm.6434, 2013b.

Lewicka-Szczebak, D., Well, R., Köster, J. R., Fuß, R., Senbayram, M., Dittert, K., and Flessa, H.: Experimental determinations of isotopic fractionation factors associated with N₂O production and reduction during denitrification in soils, *Geochim. Cosmochim. Ac.*, 134, 55–73, doi:10.1016/j.gca.2014.03.010, 2014.

Merbold, L., Eugster, W., Stieger, J., Zahniser, M., Nelson, D., and Buchmann, N.: Greenhouse gas budget (CO₂, CH₄ and N₂O) of intensively managed grassland following restoration., *Glob. Change Biol.*, 20, 1913–1928, doi:10.1111/gcb.12518, 2014.

Mohn, J., Guggenheim, C., Tuzson, B., Vollmer, M. K., Toyoda, S., Yoshida, N., and Emmenegger, L.: A liquid nitrogen-free preconcentration unit for measurements of ambient N₂O isotopomers by QCLAS, *Atmos. Meas. Tech.*, 3, 609–618, doi:10.5194/amt-3-609-2010, 2010.

Mohn, J., Tuzson, B., Manninen, A., Yoshida, N., Toyoda, S., Brand, W. A., and Emmenegger, L.: Site selective real-time measurements of atmospheric N₂O isotopomers by laser spectroscopy, *Atmos. Meas. Tech.*, 5, 1601–1609, doi:10.5194/amt-5-1601-2012, 2012.

Mohn, J., Steinlin, C., Merbold, L., Emmenegger, L., and Hagedorn, F.: N₂O emissions and source processes in snow-covered soils in the Swiss Alps, *Isot. Environ. Healt. S.*, 49, 520–531, doi:10.1080/10256016.2013.826212, 2013.

Mohn, J., Wolf, B., Toyoda, S., Lin, C. T., Liang, C. M., Brüggemann, N., Wissel, H., Steiker, A. E., Dyckmans, J., Szwek, L., Ostrom, N. E., Casciotti, K. L., Forbes, M., Giesemann, A., Well, R., Doucett, R. R., Yarnes, C. T., Ridley, A. R., Kaiser, J., and Yoshida, N.: Inter-laboratory assessment of notrous oxide isotopomer analysis of isotopomer analysis by isotope ratio mass spectrometry and laser spectroscopy: current status and perspectives, *Rapid Commun. Mass Sp.*, 28, 1995–2007, 2014.

Mosier, A., Kroeze, C., Nevison, C., Oenema, O., Seitzinger, S., and van Cleemput, O.: Closing the global N₂O budget: nitrous oxide emissions through the agricultural nitrogen cycle –

Real-time grassland N₂O isotopic signature

B. Wolf et al.

Title Page

Abstract

Introduction

Conclusions

References

Tables

Figures



Back

Close

Full Screen / Esc

Printer-friendly Version

Interactive Discussion



OECD/IPCC/IEA phase II development of IPCC guidelines for national greenhouse gas inventory methodology, *Nutr. Cycl. Agroecosys.*, 52, 225–248, 1998.

Myhre, G., Shindell, D., Bréon, F.-M., Collins, W., Fuglestvedt, J., Huang, J., Koch, D., Lamarque, L., Mendoza, B., Nakaijima, T., Robock, A., Stephens, G., Takemura, T., and Zhang, H.: Anthropogenic and natural radiative forcing, in: *Climate Change 2013: The Physical Science Basis. Contribution of Working Group I to the Fifth Assessment Report of the Intergovernmental Panel on Climate Change*, edited by: Stocker, T. F., Qin, D., Plattner, G.-K., Tignor, M., Allen, S. K., Boschung, J., Nauels, A., Xia, Y., Bex, V., and Midgley, P. M., Cambridge University Press, Cambridge, UK and New York, NY, USA, 659–740, 2013.

Ogawa, M. and Yoshida, N.: Intramolecular distribution of stable nitrogen and oxygen isotopes of nitrous oxide emitted during coal combustion, *Chemosphere*, 61, 877–887, doi:10.1016/j.chemosphere.2005.04.096, 2005.

Opdyke, M. R., Ostrom, N. E., and Ostrom, P. H.: Evidence for the predominance of denitrification as a source of N₂O in temperate agricultural soils based on isotopologue measurements, *Global Biogeochem. Cy.*, 23, 1–10, GB4018, doi:10.1029/2009GB003523, 2009.

Ostrom, N. E. and Ostrom, P. H.: The isotopomers of nitrous oxide: analytical considerations and application to resolution of microbial production pathways, in: *Handbook of Environmental Isotope Geochemistry*, vol. 1, edited by: Baskaran, M., Springer, Berlin, Heidelberg, 453–476, 2011.

Ostrom, N. E., Pitt, A., Sutka, R. L., Ostrom, P. H., Grandy, A. S., Huizinga, K. M., and Robertson, G. P.: Isotopologue effects during N₂O reduction in soils and in pure cultures of denitrifiers, *J. Geophys. Res.*, 112, 1–12, doi:10.1029/2006JG000287, 2007.

Ostrom, N. E., Sutka, R., Ostrom, P. H., Grandy, A. S., Huizinga, K. M., Gandhi, H., von Fischer, J. C., and Robertson, G. P.: Isotopologue data reveal bacterial denitrification as the primary source of N₂O during a high flux event following cultivation of a native temperate grassland, *Soil Biol. Biochem.*, 42, 499–506, doi:10.1016/j.soilbio.2009.12.003, 2010.

Park, S., Pérez, T., Boering, K. A., Trumbore, S. E., Gil, J., Marquina, S., and Tyler, S. C.: Can N₂O stable isotopes and isotopomers be useful tools to characterize sources and microbial pathways of N₂O production and consumption in tropical soils?, *Global Biogeochem. Cy.*, 25, 1–16, doi:10.1029/2009GB003615, 2011.

Real-time grassland N₂O isotopic signature

B. Wolf et al.

Title Page

Abstract

Introduction

Conclusions

References

Tables

Figures



Back

Close

Full Screen / Esc

Printer-friendly Version

Interactive Discussion



- Pataki, D., Ehleringer, J., Flanagan, L., Yakir, D., Bowling, D., Still, C., Buchmann, N., Kaplan, J., and Berry, J.: The application and interpretation of Keeling plots in terrestrial carbon cycle research, *Global Biogeochem. Cy.*, 17, 1022, doi:10.1029/2001GB001850, 2003.
- Perez, T., Trumbore, S. E., Tyler, S. C., Matson, P. A., Ortiz-Monasterio, I., Rahn, T., and Griffith, D. W. T.: Identifying the agricultural imprint on the global N₂O budget using stable isotopes, *J. Geophys. Res.*, 106, 9869–9878, 2001.
- Perez, T., Garcia-Montiel, D. C., Trumbore, S. E., Tyler, S., de Camargo, P. B., Moreira, M., Piccolo, M. C., and Cerri, C.: Nitrous oxide nitrification and denitrification ¹⁵N enrichment factors from Amazon forest soils, *Ecol. Appl.*, 16, 2153–2167, 2006.
- Ravishankara, A. R., Daniel, J. S., and Portmann, R. W.: Nitrous oxide (N₂O): the dominant ozone-depleting substance emitted in the 21st century, *Science*, 326, 123–125, doi:10.1126/science.1176985, 2009.
- Roth, K.: *Bodenkartierung und GIS-basierte Kohlenstoffinventur von Graslandböden*, University of Zürich (UZH), 132 pp., 2006.
- Saggar, S., Jha, N., Deslippe, J., Bolan, N. S., Luo, J., Giltrap, D. L., Kim, D.-G., Zaman, M., and Tillman, R. W.: Denitrification and N₂O : N₂ production in temperate grasslands: processes, measurements, modelling and mitigating negative impacts, *Sci. Total Environ.*, 465, 173–195, doi:10.1016/j.scitotenv.2012.11.050, 2013.
- Sutka, R. L., Ostrom, N. E., Ostrom, P. H., Gandhi, H., and Breznak, J. A.: Nitrogen isotopomer site preference of N₂O produced by *Nitrosomonas europaea* and *Methylococcus capsulatus* Bath., *Rapid Commun. Mass Sp.*, 17, 738–745, doi:10.1002/rcm.968, 2003.
- Sutka, R. L., Ostrom, N. E., Ostrom, P. H., Breznak, J. A., Pitt, A. J., Li, F., and Gandhi, H.: Distinguishing nitrous oxide production from nitrification and denitrification on the basis of isotopomer abundances, *Appl. Environ. Microbiol.*, 72, 638–644, doi:10.1128/AEM.72.1.638-644.2006, 2006.
- Sutka, R. L., Adams, G. C., Ostrom, N. E., and Ostrom, P. H.: Isotopologue fractionation during N₂O production by fungal denitrification, *Rapid Commun. Mass Sp.*, 22, 3989–3996, doi:10.1002/rcm, 2008.
- Syakila, A. and Kroeze, C.: The global nitrous oxide budget revisited, *Greenhouse Gas Measurement and Management*, 1, 17–26, doi:10.3763/ghgmm.2010.0007, 2011.
- Toyoda, S. and Yoshida, N.: Determination of nitrogen isotopomers of nitrous oxide on a modified isotope ratio mass spectrometer, *Anal. Chem.*, 71, 4711–4718, 1999.

Real-time grassland N₂O isotopic signature

B. Wolf et al.

Title Page

Abstract

Introduction

Conclusions

References

Tables

Figures



Back

Close

Full Screen / Esc

Printer-friendly Version

Interactive Discussion



Toyoda, S., Mutoke, H., Yamagishi, H., Yoshida, N., and Tanji, Y.: Fractionation of N₂O isotopomers during production by denitrifier, *Soil Biol. Biochem.*, 37, 1535–1545, doi:10.1016/j.soilbio.2005.01.009, 2005.

5 Toyoda, S., Yano, M., Nishimura, S., Akiyama, H., Hayakawa, A., Koba, K., Sudo, S., Yagi, K., Makabe, A., Tobari, Y., Ogawa, N. O., Ohkouchi, N., Yamada, K., and Yoshida, N.: Characterization and production and consumption processes of N₂O emitted from temperate agricultural soils determined via isotopomer ratio analysis, *Global Biogeochem. Cy.*, 25, 1–17, doi:10.1029/2009GB003769, 2011.

10 Toyoda, S., Kuroki, N., Yoshida, N., Ishijima, K., Tohjima, Y., and Machida, T.: Decadal time series of tropospheric abundance of N₂O isotopomers and isotopologues in the Northern Hemisphere obtained by the long-term observation at Hateruma Island, Japan, *J. Geophys. Res.-Atmos.*, 118, 3369–3381, doi:10.1002/jgrd.50221, 2013.

15 Tuzson, B., Zeyer, K., Steinbacher, M., McManus, J. B., Nelson, D. D., Zahniser, M. S., and Emmenegger, L.: Selective measurements of NO, NO₂ and NO_y in the free troposphere using quantum cascade laser spectroscopy, *Atmos. Meas. Tech.*, 6, 927–936, doi:10.5194/amt-6-927-2013, 2013.

Waechter, H., Mohn, J., Tuzson, B., Emmenegger, L., and Sigrist, M. W.: Determination of N₂O isotopomers with quantum cascade laser based absorption spectroscopy, *Opt. Express*, 16, 9239–9244, 2008.

20 Watts, S. H. and Seitzinger, S. P.: Denitrification rates in organic and mineral soils from riparian sites?: a comparison of N₂ flux and acetylene inhibition methods, *Soil Biol. Biochem.*, 32, 1383–1392, 2000.

Well, R. and Flessa, H.: Isotopologue enrichment factors of N₂O reduction in soils, *Rapid Commun. Mass Sp.*, 23, 2996–3002, doi:10.1002/rcm, 2009a.

25 Well, R. and Flessa, H.: Isotopologue signatures of N₂O produced by denitrification in soils, *J. Geophys. Res.*, 114, 1–11, doi:10.1029/2008JG000804, 2009b.

Well, R., Kurganova, I., Lopesdegerenyu, V., and Flessa, H.: Isotopomer signatures of soil-emitted N₂O under different moisture conditions – a microcosm study with arable loess soil, *Soil Biol. Biochem.*, 38, 2923–2933, doi:10.1016/j.soilbio.2006.05.003, 2006.

30 Well, R., Flessa, H., Xing, L., Xiaotang, J., and Römheld, V.: Isotopologue ratios of N₂O emitted from microcosms with NH₄⁺ fertilized arable soils under conditions favoring nitrification, *Soil Biol. Biochem.*, 40, 2416–2426, doi:10.1016/j.soilbio.2008.06.003, 2008.

Real-time grassland N₂O isotopic signature

B. Wolf et al.

Title Page

Abstract

Introduction

Conclusions

References

Tables

Figures



Back

Close

Full Screen / Esc

Printer-friendly Version

Interactive Discussion



Wrage, N., Velthof, G. L., van Beusichem, M. L., and Oenema, O.: Role of nitrifier denitrification in the production of nitrous oxide, *Soil Biol. Biochem.*, 33, 1723–1732, 2001.

Wu, H., Dannenmann, M. D., Wolf, B., Han, X. G., Zheng, X., and Butterbach-Bahl, K.: Seasonality of soil microbial nitrogen turnover in continental steppe soils of Inner Mongolia, *Ecosphere*, 3, 34, doi:10.1890/ES11-00188.1, 2012.

Wunderlin, P., Mohn, J., Joss, A., Emmenegger, L., and Siegrist, H.: Mechanisms of N₂O production in biological wastewater treatment under nitrifying and denitrifying conditions, *Water Res.*, 46, 1027–1037, doi:10.1016/j.watres.2011.11.080, 2012.

Wunderlin, P., Lehmann, M. F., Siegrist, H., Tuzson, B., Joss, A., Emmenegger, L., and Mohn, J.: Isotope signatures of N₂O in a mixed microbial population system: constraints on N₂O producing pathways in wastewater treatment, *Environ. Sci. Technol.*, 47, 1339–1348, doi:10.1021/es303174x, 2013.

Yamulki, S., Toyoda, S., Yoshida, N., Veldkamp, E., Grant, B., and Bol, R.: Diurnal fluxes and the isotopomer ratios of N₂O in a temperate grassland following urine amendment, *Rapid Commun. Mass Sp.*, 15, 1263–1269, doi:10.1002/rcm.352, 2001.

Yoshida, N. and Toyoda, S.: Constraining the atmospheric N₂O budget from intramolecular site preference in N₂O isotopomers, *Nature*, 405, 330–334, doi:10.1038/35012558, 2000.

Zeeman, M. J., Hiller, R., Gilgen, A. K., Michna, P., Plüss, P., Buchmann, N., and Eugster, W.: Management and climate impacts on net CO₂ fluxes and carbon budgets of three grasslands along an elevational gradient in Switzerland, *Agr. Forest Meteorol.*, 150, 519–530, doi:10.1016/j.agrformet.2010.01.011, 2010.

Real-time grassland N₂O isotopic signature

B. Wolf et al.

Title Page

Abstract

Introduction

Conclusions

References

Tables

Figures



Back

Close

Full Screen / Esc

Printer-friendly Version

Interactive Discussion



Table 1. Reference gas and compressed air tanks used during the campaign. S1 and S2 represent the anchor and calibration standard. C1 and C2 are the target gases used for determination of system performance. The reported precision is the 1σ SD.

Tank	$\delta^{15}\text{N}^{\alpha}$ [‰]	$\delta^{15}\text{N}^{\beta}$ [‰]	$\delta^{18}\text{O}$ [‰]	$\delta^{15}\text{N}^{\text{bulk}}$ [‰]	SP [‰]	mixing ratio* [ppm/ppb]
S1	15.66 ± 0.03	-3.22 ± 0.13	34.89 ± 0.05	6.22 ± 0.07	18.88 ± 0.13	90.09 ± 0.01
S2	10.38 ± 0.03	-10.55 ± 0.1	25.44 ± 0.06	-0.09 ± 0.05	20.93 ± 0.10	87.28 ± 0.003
C1	15.40 ± 0.08	-3.04 ± 0.06	43.65 ± 0.08	6.18 ± 0.05	18.44 ± 0.10	327.01 ± 0.05
C2	15.65 ± 0.17	-4.27 ± 0.08	44.20 ± 0.07	5.69 ± 0.09	19.92 ± 0.19	327.45 ± 0.05

* ppm for S1 and S2, ppb for C1, C2.

Real-time grassland N₂O isotopic signature

B. Wolf et al.

Title Page

Abstract

Introduction

Conclusions

References

Tables

Figures

◀

▶

◀

▶

Back

Close

Full Screen / Esc

Printer-friendly Version

Interactive Discussion



Table 2. Adjusted r^2 and p values for regression analysis of Keeling-plot derived isotopic compositions in soil-emitted N₂O vs. auxiliary variables N₂O flux ($f_{\text{N}_2\text{O}}$), difference of maximum and minimum concentration over a noon-to-noon period ($\Delta\text{N}_2\text{O}$), precipitation (prcp), soil moisture (wfps), soil temperature (T) and nutrient concentrations (NO_3^- , NH_4^+ and DOC).

explanatory	SP r^2	SP p	$\delta^{15}\text{N}^{\text{bulk}}$ r^2	$\delta^{15}\text{N}^{\text{bulk}}$ p	$\delta^{18}\text{O}$ r^2	$\delta^{18}\text{O}$ p	n
$f_{\text{N}_2\text{O}}$	0.14	**	0.04	0.06	0.16	**	62
$\Delta\text{N}_2\text{O}$	0.09	*	0.1	*	0.11	*	65
prcp	0.24	**	0.03	0.08	0.24	**	62
wfps	0.14	*	0.29	**	-0.009	0.52	65
T	0.22	**	0.30	**	0.12	*	65
DOC	0.23	*	0.30	*	0.03	0.23	18
NO_3^-	0.04	0.14	0.27	*	0.16	*	31
NH_4^+	-0.03	0.75	-0.03	0.89	-0.03	0.93	31

Significance codes: *: $p < 0.05$; **: $p < 0.001$. sample size (n) differs due to data availabilities.

Real-time grassland
N₂O isotopic
signature

B. Wolf et al.

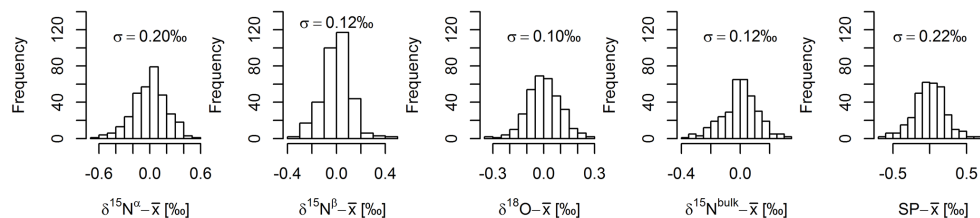


Figure 1. Repeatability (SD σ) derived by target gas injections ($n = 331$) over a 3 month period. As two target gas tanks were used, histograms show deviation of respective tank means, \bar{x} , for $\delta^{15}\text{N}^{\alpha}$, $\delta^{15}\text{N}^{\beta}$, $\delta^{18}\text{O}$, $\delta^{15}\text{N}^{\text{bulk}}$ and SP, respectively.

Title Page

Abstract

Introduction

Conclusions

References

Tables

Figures



Back

Close

Full Screen / Esc

Printer-friendly Version

Interactive Discussion



Real-time grassland N₂O isotopic signature

B. Wolf et al.

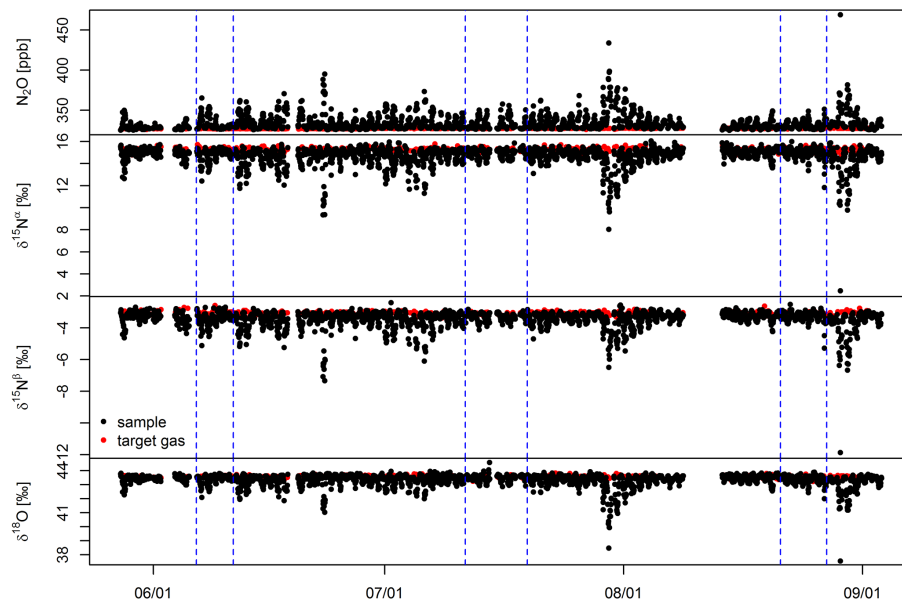


Figure 2. Target gas (red) and surface layer (black) N₂O mole fractions (top) and δ -values (three bottom panels) measured in the atmospheric surface layer in 2 m height during the field campaign. Each couple of vertical dashed blue lines indicates the management events mowing (first line) and fertilization (second line).

Title Page

Abstract

Introduction

Conclusions

References

Tables

Figures



Back

Close

Full Screen / Esc

Printer-friendly Version

Interactive Discussion



Real-time grassland N₂O isotopic signature

B. Wolf et al.

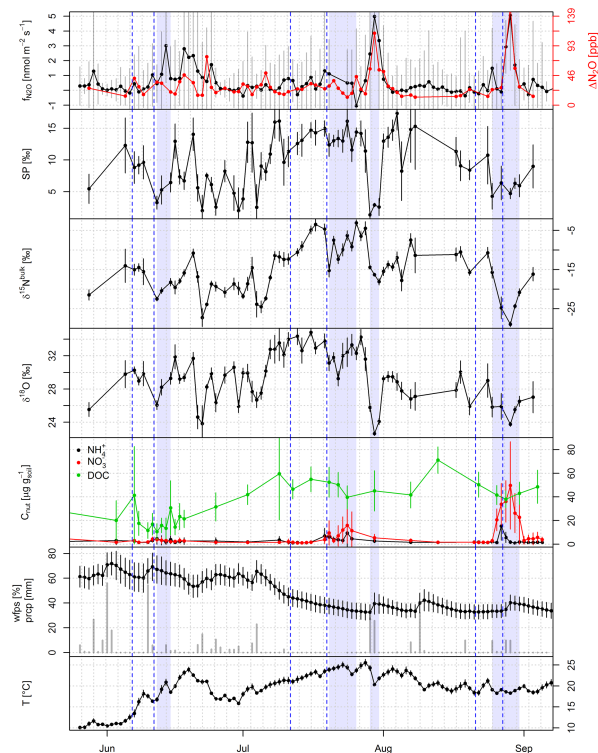


Figure 3. Noon-to-noon averaged N₂O flux ($f_{\text{N}_2\text{O}}$), overnight increase in N₂O mole fractions (difference in minimum and maximum N₂O concentration in a noon-to-noon period; $\Delta\text{N}_2\text{O}$), Keeling-plot derived isotopic composition of soil-emitted N₂O (SP, $\delta^{15}\text{N}^{\text{bulk}}$, $\delta^{18}\text{O}$), nutrient concentrations (ammonium, nitrate and dissolved organic carbon; DOC), water filled pore space (wfps), precipitation (prcp) and soil temperature (T) over the measurement period. Each couple of vertical dashed blue lines indicates the management events mowing (first line) and fertilization (second line). Transparent blue boxes represent periods of N₂O emission influenced by management or rewetting (third box).

Title Page

Abstract

Introduction

Conclusions

References

Tables

Figures



Back

Close

Full Screen / Esc

Printer-friendly Version

Interactive Discussion



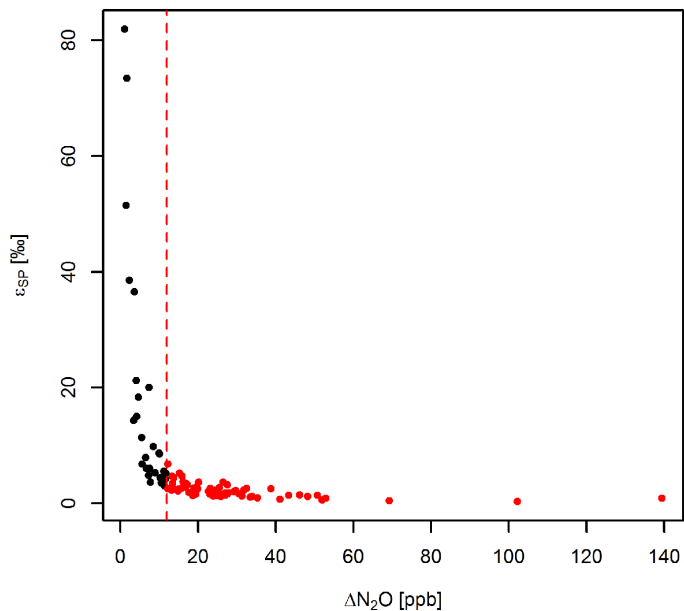


Figure 4. Standard error for SP (ϵ_{SP}) of soil-derived N_2O estimated by the Keeling plot approach as function of overnight N_2O accumulation in the surface layer. The red dashed lines show 12 ppb increase in N_2O mole fractions. Red full circles represent the selected subset.

**Real-time grassland
 N_2O isotopic
signature**

B. Wolf et al.

Title Page

Abstract

Introduction

Conclusions

References

Tables

Figures



Back

Close

Full Screen / Esc

Printer-friendly Version

Interactive Discussion



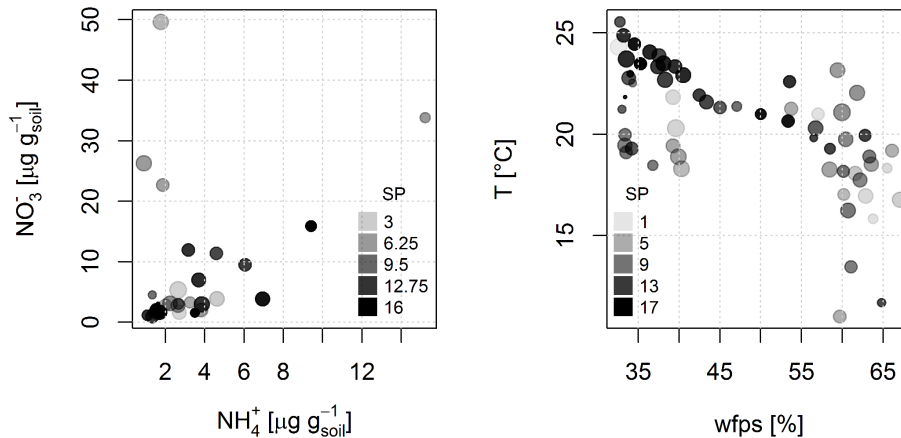


Figure 5. SP- $\text{NH}_4^+/\text{NO}_3^-$ and SP-wfps/soil temperature maps. The size of the points is inversely scaled to Keeling plot intercept standard error so that biggest points are those with lowest uncertainty.

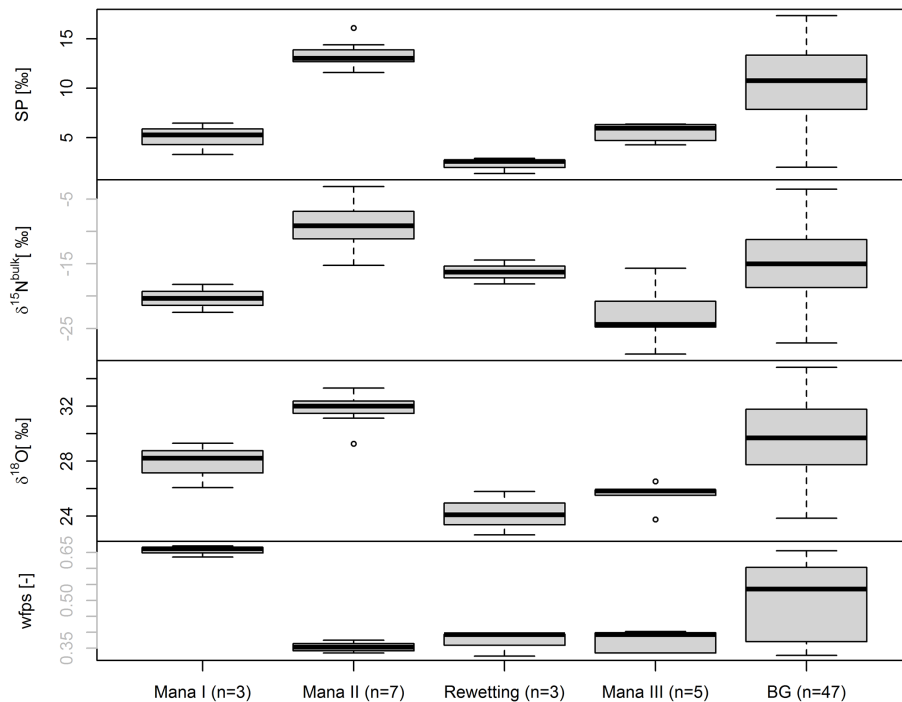


Figure 6. Boxplots for Keeling-plot derived SP, $\delta^{15}\text{N}^{\text{bulk}}$, $\delta^{18}\text{O}$ of soil-emitted N_2O and wfps of management events (Mana I–III), rainfall after a dry period (Rewetting), and the remaining measurement period (BG).

Real-time grassland N₂O isotopic signature

B. Wolf et al.

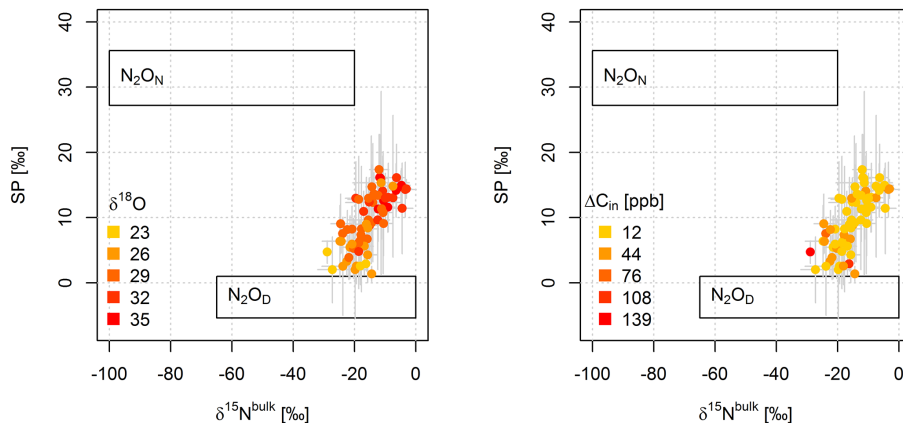


Figure 7. Map of N₂O isotopic composition with rectangles representing process groups N₂O_N and N₂O_D based on SP values in Decock and Six (2013) and δ¹⁵N^{bulk} estimated from minimum and maximum fractionation factors reported in Baggs (2008) and substrate isotopic compositions reported by Bedard-Haughn et al. (2003), Pörtl et al. (2007) and Toyoda et al. (2011).

Title Page

Abstract

Introduction

Conclusions

References

Tables

Figures

◀

▶

◀

▶

Back

Close

Full Screen / Esc

Printer-friendly Version

Interactive Discussion

